CENTRE FOR APPLIED MACROECONOMICS AND COMMODITY PRICES (CAMP)

CAMP Working Paper Series
No 12/2018

International Transmission of Macroeconomic Uncertainty in Small Open Economies: An Empirical Approach

Jamie L. Cross, Chenghan Hou and Aubrey Poon

BI NORWEGIAN BUSINESS SCHOOL

International Transmission of Macroeconomic Uncertainty in Small Open Economies: An Empirical Approach*

Jamie L. Cross
BI Norwegian Business School
Centre of Applied Macroeconomics and Commodity Prices (CAMP)
Centre for Applied Macroeconomic Analysis (CAMA)

Chenghan Hou†
Hunan University
Center for Economics, Finance and Management Studies (CEFMS)

Aubrey Poon
University of Strathclyde
Centre for Applied Macroeconomic Analysis (CAMA)

November 2018

*We thank Gary Koop, Dimitris Korobilis, Joshua Chan, Todd Clark, Benjamin Wong, Joscha Beckmann, Yiqiao Sun and members of the 12th RCEA Bayesian Workshop for their comments in the development of this research. Emails: jamie.cross@bi.no, chenghan.hou@hotmail.com, aubrey.poon@strath.ac.uk.
†Corresponding author.

Abstract

We estimate the effects of domestic and international sources of macroeconomic uncertainty in three small open economy (SOE) inflation targeting countries: Australia, Canada and New Zealand. To this end, we propose a structural VAR model with a common stochastic volatility in mean component, and develop an efficient Markov chain Monte Carlo algorithm to estimate the new model. An important feature of the model is that it allows us to test various hypotheses in an internally consistent manner. Our main result is that international uncertainty spillovers shape the macroeconomic conditions in all SOEs. The general mechanism is that international uncertainty shocks reduce real GDP, while raising inflation and interest rates. Domestic uncertainty shocks are found to have a similar effect on inflation and interest rates, however the real GDP responses are idiosyncratic. In particular, the transmission of domestic uncertainty shocks is found to be negative in Canada and positive in New Zealand, while the Australian response is initially negative and becomes positive over time. While the Canadian responses are similar to established results on the US economy, our findings highlight potentially different transmission mechanisms in Australia and New Zealand. Finally, in a forecasting exercise, we show that accounting for macroeconomic uncertainty via our model specification provides more accurate point and density forecasts compared to commonly used benchmarks.

Keywords: Bayesian VARs, International Spillovers, Small Open Economies, Stochastic Volatility in Mean, Uncertainty.

JEL-Classification: C11, C15, C53, E37, F62

1 Introduction

A recent literature has demonstrated the significance of modeling macroeconomic uncertainty in the US economy (see, among others: Bloom (2009); Mumtaz and Zanetti (2013); Born and Pfeifer (2014); Fernández-Villaverde et al. (2015); Rossi and Sekhposyan (2015); Jurado et al. (2015); Baker et al. (2016); Basu and Bundick (2017); Aastveit et al. (2017); Carriero et al. (2017); Mumtaz and Theodoridis (2017a); Bloom et al. (2018); Carriero et al. (2018); Ismailov and Rossi (2018)). As idiosyncratic shocks are the primary driver of the US business cycle, researchers tend to model the macroeconomic environment under the assumption of a closed economy. The consequence of this approach is that little is known about the effects of international uncertainty spillovers. While such information is not of first-order importance to policymakers in large economies, it is potentially important for those in small open economies (SOEs) who are highly susceptible to international shocks. For instance, Justiniano and Preston (2010) find that around half medium term Canadian output growth volatility is explained by macroeconomic shocks from the US economy. Given the known importance of international macroeconomic spillovers, and the recent interest in domestic uncertainty in the US economy, it is natural for policymakers to ask: *what are the effects of international uncertainty spillovers on SOEs*?

We address this policy-relevant question by developing a structural VAR model with a country-specific stochastic volatility in the mean component. Consistent with recent studies on the US economy, our measures of domestic macroeconomic uncertainty are defined as the common component in the second-moment of a particular country's macroeconomic variables (Jurado et al., 2015; Mumtaz and Theodoridis, 2017a; Carriero et al., 2017). Moreover, unanticipated changes in the second-moment, i.e. uncertainty shocks, are allowed to directly impact the mean dynamics of the model. This is particularly important for our research question, as it enables us to empirically test the importance of uncertainty shocks in an internally consistent manner.

Using the US as a large economy, our analysis reveals important insights on the effects of uncertainty shocks in three commonly studied inflation targeting SOEs: Australia, Canada and New Zealand[1]. Our results suggest that both domestic and foreign sources of macroeconomic uncertainty shape the economic climate in each of the SOEs. In particular, international uncertainty spillovers are found to have a persistent negative impact on real GDP, while increasing both inflation and interest rates. Domestic uncertainty shocks are found to have a similar effect on inflation and interest rates, however the real GDP responses are idiosyncratic. In particular, the transmission of domestic uncertainty shocks is negative in Canada and positive in New Zealand, while the Australian response is initially negative and becomes positive over time. This suggests that these economies exhibit different transmission mechanisms compared to the US economy. More precisely, the New Zealand experience is suggestive of *growth options* or *Oi-Hartman-Abel* effects, while the Australian response is consistent with a strong *precautionary savings* channel, which are not typically found in studies of the US economy. Given the importance of these shocks, along with the fact that each of the SOEs has an inflation targeting mandate, we then investigate whether accounting for uncertainty can generate more accurate forecasts. Indeed, we find that accounting for macroeconomic uncertainty improves the forecast performance of a conventional VAR with and without stochastic volatility. Taken together, our results suggests that macroeconomic uncertainty plays a key role in shaping the economic environments in all SOEs, and accounting for this uncertainty can aid policymakers in making better informed decisions.

In terms of empirical application, our research extends the wide literature on international macroeconomic spillovers (Schmitt-Grohé, 1998; Canova, 2005; Canova et al., 2007; Canova and Ciccarelli, 2012; Justiniano and Preston, 2010; Guerron-Quintana,

[1]We use the US as a large economy because it has recently been shown to be the main driver of global macroeconomic uncertainty (Carriero et al., 2018). The SOEs were among the first countries in the world to adopt an inflation targeting framework. Specifically, Australia adopted inflation targeting in 1992, Canada in 1991 and New Zealand in 1990.

2013; Aastveit et al., 2016; Faccini et al., 2016), and is intimately related to the small literature on international uncertainty spillovers (Caggiano et al., 2017; Cross et al., 2017; Mumtaz and Theodoridis, 2017b; Carriero et al., 2018). While our research complements each of these papers, there are key differences between them. For instance, Cross et al. (2017) employ a theoretically constrained DSGE model to quantify the effects of macroeconomic uncertainty shocks. In contrast our model allows for a more flexible empirical investigation. In this sense our paper is more similar to Mumtaz and Theodoridis (2017b) and Carriero et al. (2018), which use factor models to measure the empirical effects of international spillovers among a range of developed economies. In particular, Mumtaz and Theodoridis (2017b) consider the effects of global shocks in driving macroeconomic and financial conditions in 11 OECD countries, while Carriero et al. (2018) extend this analysis to quantify the effects of international uncertainty spillovers on two data sets: a 19-country GDP data set, and a data set with various macroeconomic variables from the US, Euro Area and the UK. In contrast, our objective in this paper is to focus on the transmission of uncertainty spillovers from large to SOEs. The present study is therefore complementary to each of these papers. In particular, the findings that (1) Australia and New Zealand exhibit different uncertainty transmission mechanisms as compared to the US economy, and that (2) accounting for uncertainty can enhance forecast accuracy, are entirely novel results.

In terms of empirical methods, our model can be viewed as a multivariate extension of the univariate stochastic volatility in mean model (SVM) of Koopman and Hol Uspensky (2002). Alternatively, it can be viewed as an extension of the common stochastic volatility model of Carriero et al. (2016), to a framework in which the time-varying second moments have first-order effects. In this manner, it is similar to the models proposed by Mumtaz and Theodoridis (2017a) and Carriero et al. (2017, 2018). In the former paper, Mumtaz and Theodoridis (2017a) develop a single factor SVM model to analyze the effects of domestic macroeconomic uncertainty shocks in the US economy. A similar

single factor framework was also used to examine uncertainty spillovers in Carriero et al. (2018)[2]. In contrast, since this paper focuses on the transmission of domestic and international uncertainty shocks, we allow the log-volatilities from both large open economy and SOE to be correlated with each other, while having direct impact on the relevant macroeconomic variables of interest. In this sense, our proposed model is most similar to the two factor SVM model in Carriero et al. (2017), who study the impact of macroeconomic and financial uncertainty shocks in the US economy. Indeed, from a purely statistical perspective our model can be viewed as a version of their framework in which we focus solely on common variation in the macroeconomic variables, as opposed to idiosyncratic volatility. Since we are interested in the effects of macroeconomic uncertainty, we believe that nothing is lost in the context to our research question. Instead, one major advantage of our proposed specification is that it allows for a development of an efficient MCMC algorithm which facilitates the testing of various economically motivated model comparison exercises, along with our forecasting exercise. Thus, a third contribution of our paper is that we develop an efficient Markov chain Monte Carlo (MCMC) based algorithm to estimate multivariate common SVM models. The key to understanding our algorithm is to note that the Hessian of the proposed log-conditional densities for the log-volatilities are band matrices. We exploit this fact by building upon recent advances in band and sparse matrix algorithms (Chan and Jeliazkov, 2009; Rue et al., 2009; McCausland et al., 2011), which have been shown to perform efficiently in the estimation of various state space models (McCausland, 2012; Chan and Grant, 2016; Chan, 2017).

The rest of this paper is structured as follows. In Section 2 we introduce the model used in the analysis and develop the efficient posterior simulator. In Sections 3 and 4 we respectively present the in- and out-of-sample results. Finally, in Section 5 we conclude.

[2]We highlight that Carriero et al. (2018) specify separate models for their two applications. First, to examine uncertainty shocks in the 19-country GDP dataset, they specify a single factor, interpreted as a global uncertainty factor. The second specification used in the 3-economy macroeconomic dataset has two factors but only one these—the global uncertainty factor—enters the models mean dynamics. Thus, in both cases the component of the common stochastic volatility in the mean dynamic is scalar valued.

2 Common Stochastic Volatility in Mean VAR

2.1 The Model

In this section we introduce the Common Stochastic Volatility in Mean VAR (CSVM-VAR) model. To set the stage, let $\mathbf{y}_t = (y_{1,t}, \ldots, y_{2n,t})' = (\mathbf{y}_t^{L'}, \mathbf{y}_t^{S'})'$ denote a vector of variables of interest, where the superscripts respectively denote the set of variables in the large and SOE. In our study, both $\mathbf{y}_t^L$ and $\mathbf{y}_t^S$ are $n \times 1$ vectors, however the model can also accommodate vectors of distinct size. The structural version of the CSVM-VAR model is given by

$$\mathbf{B}_0 \mathbf{y}_t = \mathbf{c} + \sum_{i=1}^{p} \mathbf{B}_i \mathbf{y}_{t-i} + \mathbf{A} \begin{pmatrix} e^{h_t^L} \\ e^{h_t^S} \end{pmatrix} + \boldsymbol{\epsilon}_t^y, \quad \boldsymbol{\epsilon}_t^y \sim \mathcal{N}(\mathbf{0}, \boldsymbol{\Sigma}_t), \tag{1}$$

where $\mathcal{N}(\cdot, \cdot)$ denotes the Gaussian distribution, $\mathbf{c}$ is a $2n \times 1$ vector, $\mathbf{B}_i$, $i = 1, \ldots, p$ are conditional mean coefficients of size $2n \times 2n$, $\mathbf{B}_0$ is a lower triangular "structural impact matrix" with ones on the main diagonal. The $2n \times 2$ "uncertainty impact matrix" $\mathbf{A}$ and the $2n \times 2n$ covariance matrix $\boldsymbol{\Sigma}_t$ are specified respectively as

$$\mathbf{A} = \begin{pmatrix} \mathbf{a}_{11} & \mathbf{a}_{12} \\ \mathbf{a}_{21} & \mathbf{a}_{22} \end{pmatrix} \text{ and } \boldsymbol{\Sigma}_t = \begin{pmatrix} e^{h_t^L} \boldsymbol{\Sigma}_L & \mathbf{0} \\ \mathbf{0} & e^{h_t^S} \boldsymbol{\Sigma}_S \end{pmatrix},$$

where each $\mathbf{a}_{ij}$ with $i, j = 1, 2$ is a $n \times 1$ vector and both $\boldsymbol{\Sigma}_L$ and $\boldsymbol{\Sigma}_S$ are diagonal matrices of size $n \times n$, i.e., $\boldsymbol{\Sigma}_L = \text{diag}(\sigma_{1,L}^2, \ldots, \sigma_{n,L}^2)$ and $\boldsymbol{\Sigma}_L = \text{diag}(\sigma_{n+1,S}^2, \ldots, \sigma_{2n,S}^2)$. We note that the covariance matrix $\boldsymbol{\Sigma}_t$ is changing over time, and that this time-variation is driven by the common stochastic volatilities from both the large economy $e^{h_t^L}$, and the small economy $e^{h_t^S}$. Since they capture the common component in the volatility of the country-

specific macroeconomic variables, these terms provide measures of uncertainty, and we refer to unanticipated changes in these volatilities as *uncertainty shocks*.

The state equations for the log-volatilities are assumed to follow a stationary VAR(1) process

$$\begin{pmatrix} h_t^L \\ h_t^S \end{pmatrix} = \mathbf{\Phi} \begin{pmatrix} h_{t-1}^L \\ h_{t-1}^S \end{pmatrix} + \boldsymbol{\epsilon}_t^h, \quad \boldsymbol{\epsilon}_t^h \sim \mathcal{N}(\mathbf{0}, \mathbf{\Sigma}_h), \tag{2}$$

where $\mathbf{\Phi}$ is a full 2×2 coefficient matrix and the initial condition is set to be $(h_1^L, h_1^S)' \sim \mathcal{N}(\mathbf{0}, \mathbf{V}_h)$. We allow the log-volatilities of the small and large open economies to be correlated with each other. The main reason for this modeling specification is that the assumption of the log-volatilities following an independent AR(1) process will likely result in uncertainty shocks overshooting[3]. For example, it is well documented that US uncertainty ($e_t^{h^L}$) increased during the 2008 Global Financial Crisis (Jurado et al., 2015; Carriero et al., 2017; Mumtaz and Theodoridis, 2017a). If we were to adopt an independent AR specification, then there would be no channel through which this US originated uncertainty shock can affect the level of domestic uncertainty in Canada, for example. In contrast, by specifying a VAR process, our framework allows for transmissions of such shocks. To identify the structural shocks of the uncertainty, we adopt a simple, yet economically plausible, identifying assumption. That is, uncertainty in the large economy does not respond contemporaneously to uncertainty shocks in the small economy. To be specific, we assume $\boldsymbol{\epsilon}_t^h = \mathbf{C}\mathbf{e}_t$, where $\mathbf{C}$ is a lower triangular matrix and $\mathbf{e}_t$ collects the structural shocks that follows $\mathcal{N}(\mathbf{0}, \mathbf{I}_2)$. We also note that since the uncertainty measures are estimated within the model, uncertainty shocks are, by construction, orthogonal to the VAR shocks. In this sense, our identification strategy is very similar to that in

[3]In a previous version of the paper we specified independent AR(1) processes for the state equations and showed that this is indeed the case. Since they do not add much economic value these results have been omitted from the current presentation, but are available upon request.

Carriero et al. (2017, 2018).

To complete the model specification, we assume independent prior distributions for each of the model parameters. For the measurement equation we specify Gaussian priors for the VAR coefficients and the uncertainty impact matrix $\boldsymbol{\beta} \sim \mathcal{N}(\boldsymbol{\beta}_0, \mathbf{V}_\beta)$, $\boldsymbol{\gamma} \sim \mathcal{N}(\boldsymbol{\gamma}_0, \mathbf{V}_\gamma)$, $\mathbf{a} = \text{vec}(\mathbf{A})' \sim \mathcal{N}(\mathbf{a}_0, \mathbf{V}_a)$, and inverse-Gamma priors for the variable-specific variances:

$$\sigma_{i,L}^2 \sim \mathcal{IG}(\eta_{i,L}, \omega_{i,L}), \quad i = 1, \ldots, n,$$
$$\sigma_{j,S}^2 \sim \mathcal{IG}(\eta_{j,S}, \omega_{j,S}), \quad j = n+1, \ldots, 2n.$$

For the state equation, the coefficient and covariance matrices respectively follow truncated normal and inverse-Wishart distributions:

$$\text{vec}(\boldsymbol{\Phi}') = \boldsymbol{\phi} \sim \mathcal{N}(\boldsymbol{\phi}_0, \mathbf{V}_\phi) 1(\boldsymbol{\Phi} \in A), \quad \boldsymbol{\Sigma}_h \sim \mathcal{IW}(\mathbf{S}_h, \nu_h),$$

in which $1(Q)$ is the indicator function which equals to one if statement Q is true and zero otherwise, and the set A is the region in which the VAR(1) process is stationary.

2.2 Model Comparison

It is easy to see that our proposed CSVM-VAR model nests both the traditional SVAR in Sims (1980) and the common stochastic volatility VAR (CSV-VAR) model in Carriero et al. (2016). In particular, the CSV-VAR model can be viewed as a restricted version of our CSVM-VAR with $\mathbf{A} = \mathbf{0}$ and only one common stochastic volatility component, i.e. $h_t^L = h_t^S$ for all dates $t = 1, \ldots, T$. Moreover, by making the additional restriction that $h_t^L = h_t^S = 0$ for all dates, we get the traditional SVAR. By testing whether these restrictions are supported by the data, we can readily investigate the importance of uncertainty

shocks in the proposed economies. Given that the uncertainty measures are important, we can further address our research question by imposing economically motivated restrictions on the uncertainty impact matrix $\mathbf{A}$. Exact details for these restrictions are deferred to the next section.

To test these hypothesis, we utilize a formal Bayesian model comparison method, via the *Bayes factor*—a special case of the *posterior odds ratio*. To illustrate this procedure, let M_1 and M_2 denote two arbitrary models. The posterior odds ratio for M_1 against M_2, is defined as

$$\text{PO}_{1,2} = \frac{\mathbb{P}\left(M_1|\mathbf{y^o}\right)}{\mathbb{P}\left(M_2|\mathbf{y^o}\right)},$$

where $\mathbb{P}\left(M_i|\mathbf{y^o}\right)$ denotes the conditional probability of M_i, $i = 1, 2$, given the observed data $\mathbf{y}^o = (\mathbf{y}_1^o, \ldots, \mathbf{y}_T^o)$. By the law of conditional probability, the posterior odds ratio can be written as

$$\text{PO}_{1,2} = \frac{p\left(\mathbf{y^o}|M_1\right)}{p\left(\mathbf{y^o}|M_2\right)} \times \frac{\mathbb{P}\left(M_1\right)}{\mathbb{P}\left(M_2\right)},$$

where $p\left(\mathbf{y}|M_i\right)$ and $\mathbb{P}\left(M_i\right)$ respectively denote the marginal likelihood and prior model probability for M_i, $i = 1, 2$, where the marginal likelihood is defined as

$$p(\mathbf{y^o}|M_i) = \int_{\boldsymbol{\Theta}_i} p(\mathbf{y^o}|\boldsymbol{\theta}_i, M_i) p(\boldsymbol{\theta}_i|M_i) d\boldsymbol{\theta}_i,$$

where $\boldsymbol{\theta}_i$ is a vector of the parameters in model M_i, and $\boldsymbol{\Theta}_i$ is the associated parameter space. The ratio of two such likelihoods is known as the *Bayes factor*. It can easily be seen that the posterior odds ratio reduces to the Bayes factor of M_1 against M_2, denoted $\text{BF}_{1,2}$, under the assumption of equal prior model probabilities (i.e. $\mathbb{P}\left(M_1\right) = \mathbb{P}\left(M_2\right)$). Moreover, since it is a special case of the posterior odds ratio, the Bayes factor takes on a probabilistic interpretation. For instance, if $\text{BF}_{1,2} = 2$ then M_1 is twice as likely as M_2.

One difficulty in using Bayes factor to compare models is that the analytical solution of the marginal likelihood for many non-linear models do not exist in general. Fortunately, the marginal likelihood for any model can be represented as a product of one-step-ahead predictive likelihoods evaluated at the observed data (Geweke and Amisano, 2011). That is

$$p(\mathbf{y}^{\mathbf{o}}|M_i) = p(\mathbf{y}_1^o|M_i)\prod_{t=2}^{T} p(\mathbf{y}_t^o|\mathbf{y}_1^o,\ldots,\mathbf{y}_{t-1}^o,M_i).$$

Since it requires estimating the model at each date, the computation of this one-step-ahead predictive likelihood is computationally intensive for non-linear models. To overcome this hurdle, we develop an efficient posterior sampler which we detail in the next sub-section.

2.3 Bayesian Estimation

In this section we introduce an efficient Metropolis-within-Gibbs, Markov chain Monte Carlo (MCMC) algorithm for simulating posterior draws from the CSVM-VAR model defined in equations (1) and (2). Readers who are only interested in the empirical application may skip this section and go straight to the results.

For notational convenience, let $\mathbf{y} = (\mathbf{y}_1,\ldots,\mathbf{y}_T)'$, $\mathbf{h}^L = (h_1^L,\ldots,h_T^L)'$ and $\mathbf{h}^S = (h_1^S,\ldots,h_T^S)'$. Posterior draws can be obtained by sequentially sampling from:

1. $p(\mathbf{h}^L|\mathbf{h}^S,\mathbf{A},\boldsymbol{\beta},\boldsymbol{\gamma},\boldsymbol{\Sigma}_L,\boldsymbol{\Sigma}_S,\boldsymbol{\Phi},\boldsymbol{\Sigma}_h,\mathbf{y}) = p(\mathbf{h}^L|\mathbf{h}^S,\mathbf{A},\boldsymbol{\beta},\boldsymbol{\gamma},\boldsymbol{\Sigma}_L,\boldsymbol{\Sigma}_S,\boldsymbol{\Phi},\boldsymbol{\Sigma}_h,\mathbf{y})$;
2. $p(\mathbf{h}^S|\mathbf{h}^L,\mathbf{A},\boldsymbol{\beta},\boldsymbol{\gamma},\boldsymbol{\Sigma}_L,\boldsymbol{\Sigma}_S,\boldsymbol{\Phi},\boldsymbol{\Sigma}_h,\mathbf{y}) = p(\mathbf{h}^L|\mathbf{h}^S,\mathbf{A},\boldsymbol{\beta},\boldsymbol{\gamma},\boldsymbol{\Sigma}_L,\boldsymbol{\Sigma}_S,\boldsymbol{\Phi},\boldsymbol{\Sigma}_h,\mathbf{y})$;
3. $p(\mathbf{A},\boldsymbol{\beta},\boldsymbol{\gamma}|\mathbf{h}^L,\mathbf{h}^S,\boldsymbol{\Sigma}_L,\boldsymbol{\Sigma}_S,\boldsymbol{\Phi},\boldsymbol{\Sigma}_h,\mathbf{y}) = p(\mathbf{A},\boldsymbol{\beta},\boldsymbol{\gamma}|\mathbf{h}^L,\mathbf{h}^S,\boldsymbol{\Sigma}_L,\boldsymbol{\Sigma}_S,\mathbf{y})$;
4. $p(\boldsymbol{\Sigma}_L|\mathbf{h}^L,\mathbf{h}^S,\mathbf{A},\boldsymbol{\beta},\boldsymbol{\gamma},\boldsymbol{\Sigma}_S,\boldsymbol{\Phi},\boldsymbol{\Sigma}_h,\mathbf{y}) = p(\boldsymbol{\Sigma}_L|\mathbf{h}^L,\mathbf{A},\boldsymbol{\beta},\boldsymbol{\gamma},\mathbf{y})$;
5. $p(\boldsymbol{\Sigma}_S|\mathbf{h}^L,\mathbf{h}^S,\mathbf{A},\boldsymbol{\beta},\boldsymbol{\gamma},\boldsymbol{\Sigma}_L,\boldsymbol{\Phi},\boldsymbol{\Sigma}_h,\mathbf{y}) = p(\boldsymbol{\Sigma}_S|\mathbf{h}^S,\mathbf{A},\boldsymbol{\beta},\boldsymbol{\gamma},\mathbf{y})$;

6. $p(\boldsymbol{\Sigma}_h|\mathbf{h}^L, \mathbf{h}^S, \boldsymbol{\Sigma}_L, \boldsymbol{\Sigma}_S, \mathbf{A}, \boldsymbol{\beta}, \boldsymbol{\gamma}, \boldsymbol{\Phi}, \mathbf{y}) = p(\boldsymbol{\Sigma}_h|\mathbf{h}^L, \mathbf{h}^S, \boldsymbol{\Phi})$;

7. $p(\boldsymbol{\Phi}|\mathbf{h}^L, \mathbf{h}^S, \boldsymbol{\Sigma}_L, \boldsymbol{\Sigma}_S, \mathbf{A}, \boldsymbol{\beta}, \boldsymbol{\gamma}, \boldsymbol{\Sigma}_h, \mathbf{y}) = p(\boldsymbol{\Phi}|\mathbf{h}^L, \mathbf{h}^S, \boldsymbol{\Sigma}_h)$;

The main difficulty arises in sampling from the non-standard conditional distributions of the log-volatilities in Steps 1 and 2. Since the common stochastic volatilities, $e^{h_t^S}$ and $e^{h_t^S}$, appear in both the conditional mean and the conditional variance of the model, the efficient auxiliary mixture sampler in Kim et al. (1998) cannot be applied. In recent studies examining the impact of uncertainty on the US economy, Mumtaz and Theodoridis (2017a) sample such states using the single-move Metropolis-Hasting algorithm developed in Jacquier et al. (2002), while Carriero et al. (2017, 2018) employ a particle Gibbs sampler developed in Andrieu et al. (2010). As discussed in the introduction, the major issue with these methods is that they are computationally intensive, resulting in the key model comparison and forecasting exercises becoming infeasible. To overcome this computational hurdle, we develop an efficient single-block sampler for drawing the log-volatilities in Steps 1 and 2 of the MCMC procedure. The key to understanding the algorithm is to note that the Hessian of the log-conditional densities of the proposed distribution for the log-volatilities in these steps are band matrices. Having identified this fact, we build upon recent advances in band and sparse matrix algorithms (Rue et al., 2009; Chan and Jeliazkov, 2009; McCausland et al., 2011), which have been shown to perform efficiently in the estimation of various state space models (Chan and Grant, 2016; McCausland, 2012; Chan, 2017). In what follows, we discuss how to sample from the conditional distributions in Steps 1-2 of the MCMC procedure. Since Steps 3-7 utilizes standard techniques, we defer these estimation details to Appendix A.

To sample from the conditional distribution in Step 1, first note that equation (1) can

be expressed as

$$\mathbf{y}_t = \widetilde{\mathbf{X}}_t\boldsymbol{\beta} + \mathbf{W}_t\boldsymbol{\gamma} + \mathbf{A}\begin{pmatrix} e^{h_t^L} \\ e^{h_t^S} \end{pmatrix} + \boldsymbol{\epsilon}_t^y, \quad \boldsymbol{\epsilon}_t^y \sim \mathcal{N}(\mathbf{0}, \boldsymbol{\Sigma}_t). \tag{3}$$

where $\boldsymbol{\beta} = \text{vec}([\mathbf{c}, \mathbf{B}_1, , \ldots, \mathbf{B}_p]')$, $\widetilde{\mathbf{X}}_t = \mathbf{I}_{2n} \otimes (1, \mathbf{y}'_{t-1}, \ldots, \mathbf{y}'_{t-p})$, $\boldsymbol{\gamma}$ is a vector stacking the non-zero elements in each row $\mathbf{B}_0$ and

$$\mathbf{W}_t = \begin{pmatrix} 0 & 0 & 0 & \cdots & \cdots & \cdots & 0 \\ -y_{1,t} & 0 & 0 & \cdots & \cdots & \cdots & 0 \\ 0 & -y_{1,t} & -y_{2,t} & \cdots & \cdots & \cdots & 0 \\ \vdots & \vdots & \ddots & \vdots & \cdots & \cdots & 0 \\ 0 & \cdots & \cdots & -y_{1,t} & -y_{2,t} & \cdots & -y_{2n-1,t} \end{pmatrix}.$$

It can be seen that the equation (3) above can be written as

$$\mathbf{y}_t = \widetilde{\mathbf{X}}_t\boldsymbol{\beta} + \mathbf{W}_t\boldsymbol{\gamma} + e^{h_t^L}\begin{pmatrix} \mathbf{a}_{11} \\ \mathbf{a}_{21} \end{pmatrix} + e^{h_t^S}\begin{pmatrix} \mathbf{a}_{12} \\ \mathbf{a}_{22} \end{pmatrix} + \boldsymbol{\epsilon}_t^y, \quad \boldsymbol{\epsilon}_t^y \sim \mathcal{N}(\mathbf{0}, \boldsymbol{\Sigma}_t).$$

After rearranging the equation above, we obtain

$$\widetilde{\mathbf{y}}_t = e^{h_t^L}\begin{pmatrix} \mathbf{a}_{11} \\ \mathbf{a}_{21} \end{pmatrix} + \boldsymbol{\epsilon}_t^y,$$

where

$$\widetilde{\mathbf{y}}_t = \mathbf{y}_t - \widetilde{\mathbf{X}}_t\boldsymbol{\beta} - \mathbf{W}_t\boldsymbol{\gamma} - e^{h_t^S}\begin{pmatrix} \mathbf{a}_{12} \\ \mathbf{a}_{22} \end{pmatrix}. \tag{4}$$

Thus, by a change of variable, it follows that

$$\begin{aligned} p(\mathbf{h}^L|\mathbf{h}^S, \mathbf{A}_0, \boldsymbol{\beta}, \boldsymbol{\Sigma}_L, \boldsymbol{\Sigma}_S, \rho_L, \sigma_L^2, \mathbf{y}) &\propto p(\mathbf{y}|\mathbf{h}^L, \mathbf{h}^S, \mathbf{A}_0, \boldsymbol{\beta}, \boldsymbol{\Sigma}_L, \boldsymbol{\Sigma}_S) p(\mathbf{h}^L|\rho_L, \sigma_L^2), \\ &\propto p(\widetilde{\mathbf{y}}|\mathbf{h}^L, \mathbf{h}^S, \mathbf{A}_0, \boldsymbol{\beta}, \boldsymbol{\Sigma}_L, \boldsymbol{\Sigma}_S) p(\mathbf{h}^L|\rho_L, \sigma_L^2). \end{aligned}$$

The resulting log-likelihood can then be written as $\log p(\widetilde{\mathbf{y}}|\mathbf{h}^L) = \sum_{t=1}^T \log p(\widetilde{\mathbf{y}}_t|h_t^L)$, where we have suppressed the conditional parameters except $\mathbf{h}^L$ for notational convenience. Taking a second-order Taylor expansion around $\widetilde{\mathbf{h}}^L$ yields the approximation

$$\begin{aligned} \log p(\widetilde{\mathbf{y}}|\mathbf{h}^L) &\approx \log p(\mathbf{y}|\widetilde{\mathbf{h}}^L) + (\mathbf{h}^L - \widetilde{\mathbf{h}}^L)'\mathbf{f} - \frac{1}{2}(\mathbf{h}^L - \widetilde{\mathbf{h}}^L)'\mathbf{G}(\mathbf{h}^L - \widetilde{\mathbf{h}}^L), \\ &= -\frac{1}{2}\left(\mathbf{h}^{L\prime}\mathbf{G}\mathbf{h}^L - 2\mathbf{h}^L(\mathbf{f} + \mathbf{G}\widetilde{\mathbf{h}}^L)\right) + c_1, \end{aligned}$$

where c_1 is a constant independent of $\mathbf{h}^L$, $\mathbf{f} = (f_1, \ldots, f_T)'$ and $\mathbf{G} = \text{diag}(G_1, \ldots, G_T)$, with

$$f_t = \frac{\partial}{\partial h_t^L} \log p(\widetilde{\mathbf{y}}_t|h_t^L)\Big|_{\mathbf{h}^L = \widetilde{\mathbf{h}}^L}, \quad G_t = -\frac{\partial^2}{\partial {h_t^L}^2} \log p(\widetilde{\mathbf{y}}_t|h_t^L)\Big|_{\mathbf{h}^L = \widetilde{\mathbf{h}}^L}.$$

Thus, the log-conditional density $\widetilde{\mathbf{y}}_t$ is given by

$$\log p(\widetilde{\mathbf{y}}_t|\mathbf{h}_t^L) = -\frac{nh_t^L}{2} - \frac{1}{2}e^{-h_t^L}\left(\widetilde{\mathbf{y}}_{1,t} - e^{h_t^L}\mathbf{a}_{11}\right)'\boldsymbol{\Sigma}_L^{-1}\left(\widetilde{\mathbf{y}}_{1,t} - e^{h_t^L}\mathbf{a}_{11}\right), \tag{5}$$

$$- \frac{1}{2}e^{-h_t^S}\left(\widetilde{\mathbf{y}}_{2,t} - e^{h_t^L}\mathbf{a}_{21}\right)'\boldsymbol{\Sigma}_S^{-1}\left(\widetilde{\mathbf{y}}_{2,t} - e^{h_t^L}\mathbf{a}_{21}\right). \tag{6}$$

It is easy to check that

$$\frac{\partial}{\partial h_t^L}\log p(\widetilde{\mathbf{y}}_t|h_t^L) = -\frac{1}{2}\left(n - e^{-h_t^L}\widetilde{\mathbf{y}}_{1,t}'\boldsymbol{\Sigma}_L^{-1}\widetilde{\mathbf{y}}_{1,t} + e^{h_t^L}\mathbf{a}_{11}'\boldsymbol{\Sigma}_L^{-1}\mathbf{a}_{11}\right) + e^{h_t^L - h_t^S}\widetilde{\mathbf{y}}_{2,t}'\boldsymbol{\Sigma}_S^{-1}\mathbf{a}_{21} - e^{2h_t^L - h_t^S}\mathbf{a}_{21}'\boldsymbol{\Sigma}_S^{-1}\mathbf{a}_{21}, \tag{7}$$

$$\frac{\partial^2}{\partial {h_t^L}^2}\log p(\widetilde{\mathbf{y}}_t|h_t^L) = -\frac{1}{2}\left(e^{-h_t^L}\widetilde{\mathbf{y}}_{1,t}'\boldsymbol{\Sigma}_L^{-1}\widetilde{\mathbf{y}}_{1,t} + e^{h_t^L}\mathbf{a}_{11}'\boldsymbol{\Sigma}_L^{-1}\mathbf{a}_{11}\right) + e^{h_t^L - h_t^S}\widetilde{\mathbf{y}}_{2,t}'\boldsymbol{\Sigma}_S^{-1}\mathbf{a}_{21} - 2e^{2h_t^L - h_t^S}\mathbf{a}_{21}'\boldsymbol{\Sigma}_S^{-1}\mathbf{a}_{21}. \tag{8}$$

Next, the log conditional prior density for $\mathbf{h}^L$ is given by

$$\log p(\mathbf{h}^L|\mathbf{h}^S) = \log c_2 + \log p(h_1^L|h_1^S) + \sum_{t=2}^{T}\log p(h_t^L, h_{t-1}^L|h_t^S, h_{t-1}^S),$$

where c_2 is the normalization constant that is independent of $\mathbf{h}^L$. To derive the first and second order conditions respective to $\mathbf{h}^L$, we first rewrite the equation (2) as

$$\begin{pmatrix} -\phi_{1,1} & 1 \\ -\phi_{2,1} & 0 \end{pmatrix}\begin{pmatrix} h_{t-1}^L \\ h_t^L \end{pmatrix} = \begin{pmatrix} \phi_{1,2} & 0 \\ \phi_{2,2} & 1 \end{pmatrix}\begin{pmatrix} h_{t-1}^S \\ h_t^S \end{pmatrix} + \boldsymbol{\epsilon}_t^h, \quad \boldsymbol{\epsilon}_t^h \sim \mathcal{N}(\mathbf{0}, \boldsymbol{\Sigma}_h).$$

which implies that

$$\begin{pmatrix} h_{t-1}^L \\ h_t^L \end{pmatrix} = \boldsymbol{\mu}_t^L + \widetilde{\boldsymbol{\epsilon}}_t^h, \quad \widetilde{\boldsymbol{\epsilon}}_t^h \sim \mathcal{N}(\mathbf{0}, \boldsymbol{\Omega}_L^{-1}),$$

where

$$\boldsymbol{\mu}_t^L = \begin{pmatrix} -\phi_{1,1} & 1 \\ -\phi_{2,1} & 0 \end{pmatrix}^{-1}\begin{pmatrix} \phi_{1,2} & 0 \\ \phi_{2,2} & 1 \end{pmatrix}\begin{pmatrix} h_{t-1}^S \\ h_t^S \end{pmatrix}, \quad \boldsymbol{\Omega}_L = \begin{pmatrix} -\phi_{1,1} & 1 \\ -\phi_{2,1} & 0 \end{pmatrix}'\boldsymbol{\Sigma}_h^{-1}\begin{pmatrix} -\phi_{1,1} & 1 \\ -\phi_{2,1} & 0 \end{pmatrix},$$

then it can be shown that

$$\log p(h_t^L, h_{t-1}^L | h_t^S, h_{t-1}^S) = \log c_3 - \frac{1}{2}\left[\begin{pmatrix} h_{t-1}^L \\ h_t^L \end{pmatrix} - \boldsymbol{\mu}_t^L\right]' \boldsymbol{\Omega}_L \left[\begin{pmatrix} h_{t-1}^L \\ h_t^L \end{pmatrix} - \boldsymbol{\mu}_t^L\right],$$

where again c_3 is a normalization constant. It can be seen that

$$\begin{pmatrix} \frac{\partial}{\partial h_t} \log p(h_t^L, h_{t-1}^L | h_t^S, h_{t-1}^S) \\ \frac{\partial}{\partial h_{t-1}} \log p(h_t^L, h_{t-1}^L | h_t^S, h_{t-1}^S) \end{pmatrix} = \boldsymbol{\Omega}_L \left[\boldsymbol{\mu}_t^L - \begin{pmatrix} h_{t-1}^L \\ h_t^L \end{pmatrix}\right],$$

$$\begin{pmatrix} \frac{\partial^2}{\partial h_t^2} \log p(h_t^L, h_{t-1}^L | h_t^S, h_{t-1}^S) & \frac{\partial^2}{\partial h_t \partial h_{t-1}} \log p(h_t^L, h_{t-1}^L | h_t^S, h_{t-1}^S) \\ \frac{\partial^2}{\partial h_t \partial h_{t-1}} \log p(h_t^L, h_{t-1}^L | h_t^S, h_{t-1}^S) & \frac{\partial^2}{\partial h_{t-1}^2} \log p(h_t^L, h_{t-1}^L | h_t^S, h_{t-1}^S) \end{pmatrix} = -\boldsymbol{\Omega}_L.$$

Given the first and second order conditions above, using again the second-order Taylor expansion around $\widetilde{\mathbf{h}}^L$ to approximate the log conditional prior density gives

$$\log p(\mathbf{h}^L | \mathbf{h}^S) \approx (\mathbf{h}^L - \widetilde{\mathbf{h}}^L)' \widetilde{\mathbf{f}} - \frac{1}{2}(\mathbf{h}^L - \widetilde{\mathbf{h}}^L)' \widetilde{\mathbf{G}} (\mathbf{h}^L - \widetilde{\mathbf{h}}^L), \tag{9}$$

$$= -\frac{1}{2}\left(\mathbf{h}^{L\prime} \widetilde{\mathbf{G}} \mathbf{h}^L - 2\mathbf{h}^L (\widetilde{\mathbf{f}} + \widetilde{\mathbf{G}} \widetilde{\mathbf{h}}^L)\right) + c_4, \tag{10}$$

where

$$\widetilde{\mathbf{f}} = \begin{pmatrix} \widetilde{f}_1 \\ \widetilde{f}_2 \\ \vdots \\ \vdots \\ \widetilde{f}_T \end{pmatrix}, \quad \widetilde{\mathbf{G}} = \begin{pmatrix} \widetilde{G}_{1,1} & \widetilde{G}_{1,2} & 0 & \cdots & 0 \\ \widetilde{G}_{1,2} & \widetilde{G}_{2,2} & \widetilde{G}_{2,3} & \cdots & 0 \\ \vdots & \ddots & \ddots & \ddots & \vdots \\ 0 & \cdots & \widetilde{G}_{T-2,T-1} & \widetilde{G}_{T-1,T-1} & \widetilde{G}_{T,T-1} \\ 0 & \cdots & 0 & \widetilde{G}_{T,T-1} & \widetilde{G}_{T,T} \end{pmatrix}$$

with

$$\widetilde{f}_1 = \frac{\partial}{\partial h_1} \log p(h_2^L, h_1^L | h_2^S, h_1^S)\Big|_{\mathbf{h}^L = \widetilde{\mathbf{h}}^L} - |\mathbf{V}_h|^{-1} \left(\mathbf{V}_h(2,2)\widetilde{h}_1^L - \mathbf{V}_h(1,2)\widetilde{h}_1^S \right),$$
$$\widetilde{G}_{1,1} = -\frac{\partial^2}{\partial h_t^2} \log p(h_t^L, h_{t-1}^L | h_t^S, h_{t-1}^S)\Big|_{\mathbf{h}^L = \widetilde{\mathbf{h}}^L} + \mathbf{V}_h^{-1}(1,1).$$

The $\mathbf{U}(i,j)$ denotes the $(i,j)th$ entry in matrix $\mathbf{U}$. For $t = 2, \ldots, T$,

$$\widetilde{f}_t = \left(\frac{\partial}{\partial h_t} \log p(h_t^L, h_{t-1}^L | h_t^S, h_{t-1}^S) + \frac{\partial}{\partial h_t} \log p(h_{t+1}^L, h_t^L | h_{t+1}^S, h_t^S) \right) \Big|_{\mathbf{h}^L = \widetilde{\mathbf{h}}^L},$$
$$\widetilde{G}_{t,t} = -\left(\frac{\partial^2}{\partial h_t^2} \log p(h_t^L, h_{t-1}^L | h_t^S, h_{t-1}^S) + \frac{\partial^2}{\partial h_t^2} \log p(h_{t+1}^L, h_t^L | h_{t+1}^S, h_t^S) \right) \Big|_{\mathbf{h}^L = \widetilde{\mathbf{h}}^L}$$
$$\widetilde{G}_{t,t+1} = \mathbf{\Omega}_L(2,1).$$

Combining the log-likelihood in equation (6) with the log-prior density in equation (9) gives an approximation of the log-posterior distribution

$$\begin{aligned} \log p(\mathbf{h}^L | \mathbf{h}^S, \mathbf{y}) &= \log p(\widetilde{\mathbf{y}} | \mathbf{h}^L, \mathbf{h}^S) + \log p(\mathbf{h}^L | \mathbf{h}^S), \\ &= -\frac{1}{2} \left(\mathbf{h}^{L\prime} \mathbf{K}_\mathbf{h} \mathbf{h}^L - 2\mathbf{h}^{L\prime} \mathbf{k}_\mathbf{h} \right) + c_5, \end{aligned}$$

where c_5 is a constant that is independent of $\mathbf{h}^L$, $\mathbf{K}_\mathbf{h} = \mathbf{G} + \widetilde{\mathbf{G}}$ and $\mathbf{k}_\mathbf{h} = \mathbf{f} + \widetilde{\mathbf{f}} + \mathbf{K}_\mathbf{h}\widetilde{\mathbf{h}}$.

It can be seen that the above equation is the log-kernel of the Gaussian distribution. To implement Step 1, we first set $\widetilde{\mathbf{h}}^L$ to be the mode of the distribution $p(\mathbf{h}^L | \mathbf{h}^S, \mathbf{A}, \boldsymbol{\beta}, \boldsymbol{\gamma}, \mathbf{\Sigma}_L, \mathbf{\Sigma}_S, \mathbf{\Phi}, \mathbf{\Sigma}_h, \mathbf{y}$ which can be obtained by applying the Newton-Raphson method. The resulting Gaussian distribution $\mathcal{N}(\widetilde{\mathbf{h}}^L, \widetilde{\mathbf{K}}_\mathbf{h}^{-1})$ is then used as our proposal in the acceptance-rejection Metropolis-Hastings step, where $\widetilde{\mathbf{K}}_\mathbf{h}$ is the $\mathbf{K}_\mathbf{h}$ evaluated at $\widetilde{\mathbf{h}}^L$[4].

Since Step 2 is symmetric to Step 1, sampling can be accomplished through straight

[4]As seen in equation (8), there is no guarantee that $\widetilde{\mathbf{K}}_\mathbf{h}$ is a positive definite matrix. To overcome this problem we adopt the following strategy: First, we initialize $\widetilde{\mathbf{K}}_\mathbf{h}$ as an identity matrix. Next, in each MCMC iteration, we check whether the proposed Hessian $\widetilde{\mathbf{K}}_\mathbf{h}$ is positive definite. If it is, then we use it in the proposal distribution, otherwise we use the $\widetilde{\mathbf{K}}_\mathbf{h}$ from the previous MCMC iteration.

forward relabeling of terms in the above equations. We close by making a few remarks on the computation. First, in contrast to the multi-move samplers used in existing studies, our common stochastic volatilities are drawn in a single-block sampler. In general, single-block samplers have been proven to be more numerically efficient than single-move sampler when the posterior samples are highly correlated. Second, due to the availability of the first and second order derivatives of the log-conditional density, the Newton-Raphson method can be used to obtain the mode of the log-density efficiently. This idea is similar to the single-block version of Shephard and Pitt (1997) and Chan (2017) in that the proposal distribution in the Acceptance-Rejection MH algorithm is based on the second-order Taylor expansion of the likelihood function in terms of stochastic volatilities. Of course, they are different in that we consider a multivariate model and exploit techniques from band and sparse matrix algorithms. Specifically, since the precision matrix $\widetilde{\mathbf{K}}_{\mathbf{h}}$ is a band matrix, we can efficiently draw from the proposal distribution by applying the precision sampler in Chan and Jeliazkov (2009)[5].

3 Empirical Results

In this section we present our main empirical results on the effects of macroeconomic uncertainty in three commonly studied SOEs: Australia, Canada and New Zealand. The data for each country consists of quarterly data on real GDP, CPI inflation and a short-term interest rate—taken to be the country's bank-rate—from 1978Q3-2016Q4. All series were sourced from the International Monetary Fund's (IMF's) International Financial Statistics (IFS) database, and we convert both real GDP and CPI indexes to annualized growth measures. To maintain consistency with the broader uncertainty literature, we

[5]The attentive reader will note that we have referred to two distinct notions of efficiency here. The first refers to reduced autocorrelation in the posterior draws. The second refers to sampling speed. For this particular model, our proposed algorithm is superior to existing samplers it that it is efficient in both respects.

select a lag length $p = 2$ for the VAR coefficients (Caggiano et al., 2017; Carriero et al., 2017; Mumtaz and Theodoridis, 2017b; Carriero et al., 2018). All estimates are based on 50000 posterior draws after a burnin period of 5000. The priors are discussed in Appendix A.

3.1 Hypothesis Testing via Model Selection

In this section, we conduct a model comparison exercise using the marginal likelihood as a selection criterion. The main objective is to provide some statistical evidence that helps determine whether uncertainty plays a role in shaping the macroeconomic environments of the countries in question. To this end, we focus on the two major issues concerned in this paper. First, we question whether allowing the macroeconomic variables in a specific country to share a common volatility is consistent with the data. Second, we investigate the relevance of domestic and international sources of uncertainty within each of the SOEs. To that end, we impose four economically motivated restrictions on the impact matrix $\mathbf{A}$. To ease exposition, recall that

$$\mathbf{A} = \begin{pmatrix} \mathbf{a}_{11} & \mathbf{a}_{12} \\ \mathbf{a}_{21} & \mathbf{a}_{22} \end{pmatrix}.$$

The restrictions are: (1) $\mathbf{a}_{12} = \mathbf{0}$; (2) $\mathbf{a}_{21} = \mathbf{0}$; (3) $\mathbf{a}_{12} = \mathbf{a}_{21} = \mathbf{0}$; (4) $\mathbf{a}_{12} = \mathbf{a}_{22} = \mathbf{0}$. Restriction (1) hypothesizes that uncertainty spillovers in the SOE do not transmit to the large economy; restriction (2) that uncertainty spillovers in the large economy do not transmit to the small economy; restriction (3) that uncertainty is purely idiosyncratic (i.e. no spillovers); restriction (4) that the only source of global uncertainty is from the large economy. We summarize each of the model specifications in Table 1 and the estimated marginal likelihood of each model are reported in Table 2.

Table 1: A list of models.

VAR	constant VAR
CSV-VAR	with common SV
CSVM-VAR	with common SVM
CSVM-VAR-R1	with common SVM with $\mathbf{a}_{12} = \mathbf{0}$
CSVM-VAR-R2	with common SVM with $\mathbf{a}_{21} = \mathbf{0}$
CSVM-VAR-R3	with common SVM with $\mathbf{a}_{12} = \mathbf{a}_{21} = \mathbf{0}$
CSVM-VAR-R4	with common SVM with $\mathbf{a}_{12} = \mathbf{a}_{22} = \mathbf{0}$

The general conclusion is that the log marginal likelihoods provide overwhelming support in favor of the unrestricted CSVM-VAR model against the VAR, CSV-VAR and restricted CSVM-VAR models across all countries. In the first instance we thus conclude that there is a statistically relevant country-specific common component in the macroeconomic variables of interest. For instance, in the case of Australia, the data suggest that the CSV-VAR is approximately 57 times more likely than the traditional VAR model given the data[6]. Finally, the fact that the unrestricted CSVM-VAR model is preferred to the CSV-VAR and each of the restricted CSVM-VARs suggests that both domestic and international sources of macroeconomic uncertainty are a key feature of the economic environment in each of the SOEs.

[6]To see this note that the log Bayes factor is approximately 57 (i.e. $-932.83 - (-990.02)$).

Table 2: Estimated log marginal likelihoods for various models in Table 1.

	Australia	Canada	New Zealand
VAR	−990.02	−923.65	−1187.20
CSV-VAR	−932.83	−889.78	−1077.74
CSVM-VAR	**−920.24**	**−874.55**	**−1045.58**
CSVM-VAR-R1	−931.26	−878.28	−1052.43
CSVM-VAR-R2	−922.12	−874.66	−1063.20
CSVM-VAR-R3	−934.46	−875.83	−1059.59
CSVM-VAR-R4	−925.28	−879.11	−1055.71

Note: The best model for each country is in bold.

3.2 Uncertainty Measures

Having identified the significance of both domestic and international sources of uncertainty across each of the SOEs, we now discuss the qualitative behavior of the uncertainty measures. Figures 1 and 2 respectively present the estimated macroeconomic uncertainty index for the US and the SOEs. In each plot, the blue line represents the posterior means, and the red lines represent the associated 90% credible intervals.

If the model is well-specified, then all three versions of estimated US uncertainty measures should be similar to each other. The plots in Figure 1 show that the qualitative behavior of the resulting measures are almost identical across the three panels. We are therefore confident that the model is well-specified[7]. Moreover, the general pattern of the US uncertainty measures is consistent with those in Carriero et al. (2017). In particular,

[7]Since the actual index value has no economic interpretation, we are not concerned about the quantitative differences in these figures across estimates.

they show significant increases around some of the political and economic events that were first highlighted in Bloom (2009). For instance, uncertainty is high in the 1980s and then declines, with some spikes around the time of the Gulf War around 1990s and the "Dot-Com bubble" in the early 2000s. The index also captures the uncertainty upturn surrounding the 2008 Global Financial Crisis.

As for the SOEs, the first plot in Figure 2 shows that uncertainty in Australia increases following the 1979 energy crisis, before declining after the movement to a flexible exchange rate regime in 1983. Interestingly, the adoption of inflation targeting around 1992/93 seems to coincide with the stabilization of uncertainty over the next two decades. The notable spike in the early 2000s likely relates to the "Dot-Com bubble". Finally, there is no spike around the 2008 Global Financial Crisis. While this would be worrying for Canada or the US, the Australian economy was not significantly hit by the crisis and did not enter a recession. It is therefore plausible that the cause of uncertainty around that time were not domestic macroeconomic conditions, but instead spillovers from the US.

Similar to Australia, uncertainty in Canada increases following the 1979 energy crisis before returning to baseline by the mid-1980s. The index then peaks again around the 1990 recession before steadily declining after the adoption of inflation targeting in 1991. As in the Australian case, the notable spike in the early 2000s likely relates to the "Dot-Com bubble". In contrast to the Australian case, there is a spike in uncertainty during the GFC, however it is clear that most of the uncertainty during that period stemmed from the US economy.

Finally, the New Zealand experience is distinct from the similar fluctuations in both Australia and Canada. In particular, aside from the peak in uncertainty around 1985 the index seems to exhibit a constant mean, with a relatively minor increase around the 2008 crisis. The large spike in the mid-1980s is associated with the nine month long recession in 1982-83 and the year long recession of 1987-88 recessions. Finally, as in the case of

Australia and Canada, a possible explanation of the post-1980s reduction in uncertainty is the adoption of inflation targeting in the early 1990s.

3.3 Transmission of Uncertainty Shocks

How do macroeconomic uncertainty shocks effect the SOEs? To answer this question, we first discuss the estimated uncertainty impact matrix for each country. This is useful as it highlights the sign and size of the initial movement elicited by the uncertainty shocks. In this sense, we can measure the *direct effects* of both domestic and international sources of uncertainty shocks. Next, we analyze generalized impulse response functions (GIRFs) to a one standard deviation uncertainty shock[8]. GIRFs are useful as they provide information about how the uncertainty shock propagates throughout the economy. In this sense, we can also measure the *transmission* of the uncertainty shocks.

The posterior means and the corresponding 90% credible intervals of the impact matrix for each country are presented in Table 3. The columns of the table respectively represent the impact of US and SOE uncertainty shocks, while the rows represent the various macroeconomic variables in the SOEs: real GDP growth, CPI inflation and interest rate.

Table 3: Estimated **A** matrix for the CSVM-VAR.

Country	Variable	Posterior mean	90% Credible Interval	Posterior mean	90% Credible Interval
Australia	GDP:	-0.87	$(-2.88, 0.77)$	1.28	$(-0.05, 3.65)$
	Inflation:	0.11	$(-0.05, 0.39)$	-0.12	$(-0.48, 0.08)$
	Interest rate:	-0.16	$(-1.10, 0.51)$	0.12	$(-0.94, 1.12)$
Canada	GDP:	0.52	$(-2.74, 3.86)$	1.32	$(-2.44, 5.17)$
	Inflation:	0.05	$(-0.06, 0.22)$	-0.06	$(-0.25, 0.06)$
	Interest rate:	0.28	$(-1.90, 2.72)$	4.53	$(1.06, 8.45)$
New Zealand	GDP:	-0.33	$(-1.54, -0.02)$	0.83	$(0.09, 3.92)$
	Inflation:	0.76	$(-0.10, 2.47)$	-1.22	$(-3.74, 0.00)$
	Interest rate:	-0.15	$(-0.68, -0.01)$	0.06	$(-0.09, 0.40)$

[8]Since the measures of uncertainty are time varying, we follow Koop et al. (1996) and compute GIRFs. The difference between GIRFs and traditional IRFs, is that future shocks are not "zeroed-out" by assumption, but instead "integrated-out" through a Monte Carlo integration procedure, details which are provided in Koop et al. (1996).

A few general observations can be made. First, in line with the broad literature on the US economy, we find that US originated uncertainty shocks tend to decrease output while increasing inflation and interest rates (Born and Pfeifer, 2014; Mumtaz and Theodoridis, 2015; Carriero et al., 2017; Mumtaz and Theodoridis, 2017a). In particular, international uncertainty spillovers decrease output in both Australia and New Zealand, while increasing inflation in all countries. In contrast, such shocks lead to monetary expansions in Australia and New Zealand. While these results are novel for to our study, the Australian and New Zealand experience are consistent with the UK responses to US uncertainty shocks in Mumtaz and Theodoridis (2015). Importantly, the same result does not hold for Canada. In that case, international uncertainty spillovers increase both output and interest rates. Finally, domestic uncertainty shocks in the SOEs are found to elicit different impacts compared to international uncertainty shocks. Specifically, such shocks are found to increase real GDP and interest rates in each country, while decreasing inflation.

While the result that uncertainty induces a positive output response may seem perplexing, Bloom (2014) proposes three potential mechanisms that could be at play. The first possible explanation is that these economies each exhibits a strong *precautionary savings channel*. The precautionary savings hypothesis asserts that higher uncertainty elicits a short run reduction in consumption expenditure which results in an economic contraction. In time however, greater savings allows for higher investment which could then benefit long run growth (Bansal and Yaron, 2004; Basu and Bundick, 2017). Next, the *growth options* channel asserts that uncertainty can encourage investment if it increases potential returns. For instance, in the literature on oil drilling incentives, higher uncertainty has been shown to increase the value of call options, thus increasing the companies' value and their willingness to invest (Paddock et al., 1988). Finally, a related channel is *Oi-Hartman-Abel effects* (Abel, 1983; Hartman, 1972; Oi, 1961). This effect suggests that if firms can insure against bad outcomes then they may be risk-loving,

which result in higher investment and short run growth.

To further investigate the existence of such channels we now examine the transmission of such shocks. To that end, we plot the GIRFs in Figures 3 and 4. In each figure, the solid line represents the average mean point estimates to a (time-varying) one-standard deviation shock to the log uncertainty measures. The shaded regions are 16th and 84th percentiles of the responses. The horizontal axis represents an impulse horizon of 20 quarters (5 years), while the vertical axis displays percentage point changes.

The responses in Figure 3 show that the transmission of international uncertainty spillovers from the US are qualitatively similar across each of the SOEs. That is, the rise in US uncertainty induces persistent declines in GDP, while increasing inflation and interest rates in each country. This is interesting because our earlier examination of the uncertainty impact matrix suggested that the initial Canadian real GDP response was positive. Thus, after accounting for the full transmission mechanism we conclude that Canada does not exhibit any of the aforementioned channels that generate positive growth; at least in response to international uncertainty spillovers. Before discussing the effects of domestic uncertainty shocks, we highlight that the magnitude of the responses to international uncertainty shocks differs across the economies. In particular, the output response in Australia and New Zealand are about half the size of that in Canada. Conversely, the medium run inflation response in these countries is about twice as large as that in Canada. Given that these countries engages in inflation targeting, the positive inflation responses suggest that policymakers should take such shocks into consideration when making interest rate decisions.

Interestingly, Figure 4 shows that domestic uncertainty shocks elicit different responses relative to their international counterparts. In particular, while such shocks generate a positive inflation and interest rate response in each of the SOEs, the real GDP responses are idiosyncratic. For instance, the response in Canada is initially positive but then be-

comes persistently negative over time. In contrast, the New Zealand response is positive with no subsequent overshooting, and the Australian response is initially negative but then becomes positive over time. This suggests that each country has a different transmission mechanism for domestic uncertainty shocks, at least with respect to output. In particular, the responses in New Zealand are potentially consistent with growth options and Oi-Hartman-Abel effects, while the Australian response is consistent with a precautionary savings channel. Of course, the empirical model used in this paper is not able to address the issue of the underlying behavioral foundations of these policy changes since a Lucas (1976) critique issue arises in this type of counterfactual analysis. It is therefore not pursued in this paper, but highlights an important area of future research.

4 Forecasting

The results in the previous section suggest that uncertainty plays a key role in shaping the macroeconomic environments in all SOEs. Given the importance of these shocks, along with the fact that each of the SOEs has an inflation targeting mandate, an important question is: *can accounting for uncertainty improve the forecast accuracy of traditional econometric models*? To address this question, we compare the point and density forecast accuracy of the CSVM-VAR compared to the VAR and CSV-VAR specifications. In this exercise, we evaluate the iterated h-step-ahead forecast of each model with $h = 1, 2, 4, 8$, and the forecast evaluation period is from 1990Q1 - 2016Q4. We note that this sample is roughly equal to the period in which each country adopted inflation targeting. Thus, our exercise resembles that of the forecasting departments in the respective countries' central banks.

To assess the point forecast accuracy we report both the root mean squared forecast

error (RMSFE) and the mean absolute forecast error (MAFE):

$$\text{RMSFE} = \sqrt{\frac{\sum_{t=t_0}^{T-h} \left(\mathbf{y}_{t+h}^o - \mathbb{E}(\mathbf{y}_{t+h}|\mathbf{y}_{1:t})\right)^2}{T-h-t_0+1}},$$

$$\text{MAFE} = \frac{\sum_{t=t_0}^{T-h} \left|\mathbf{y}_{t+h}^o - \hat{\mathbf{y}}_{t+h}^M\right|}{T-h-t_0+1},$$

where $\mathbb{E}(\mathbf{y}_{t+h}|\mathbf{y}_{1:t})$ is the posterior mean of the predictive density and $\hat{\mathbf{y}}_{t+h}^M$ is the posterior median of the predictive density.

To assess the density forecast accuracy, we report the average log-predictive likelihoods (ALPL) and the average continuous rank probability score (ACRPS):

$$\text{ALPL} = \frac{\sum_{t=t_0}^{T-k} \log p_{t+h}(\mathbf{y}_{t+k} = \mathbf{y}_{t+h}^o|\mathbf{y}_1^o, \ldots, \mathbf{y}_{t-1}^o)}{T-h-t_0+1},$$

$$\text{ACRPS} = \frac{1}{T-h-t_0+1} \sum_{t=t_0}^{T-h} \text{CRPS}_t,$$

where $\text{CRPS}_t = \int_{-\infty}^{\infty} \left(F_{t+h}(z) - 1(\mathbf{y}_{t+h}^o < z)\right)^2 dz = \mathbb{E}_{p_{t+h}}|\mathbf{y}_{t+h} - \mathbf{y}_{t+h}^o| - 0.5\mathbb{E}_{p_{t+h}}|\mathbf{y}_{t+h} - \mathbf{y}_{t+h}'|$ and F_{t+h} is the cumulative distribution of the predictive density at time $t+h$ given all information up to time t. A small value of the ACRPS indicates a better forecasting performance.

The point and density forecast results for each country are reported across Tables 4-6. To facilitate comparison, we report relative scores to a VAR benchmark. Set in this manner, a relative RMSFE, MAFE and ACRPS of less than one indicates that the given

model provides a better forecast than the VAR benchmark. Conversely, a positive value for the relative ALPL indicates a better forecasting performance than the benchmark.

The general trend is that the CSVM-VAR forecasts better than the alternatives. Two notable exceptions are the point forecasts of Canadian interest rates and New Zealand real GDP. In the former case, the CSV-VAR provides the best point forecasts at all forecast horizons, however the CSVM-VAR provides better density forecasts at short-term horizons under the ALPS metric. In the latter case, the CSVM-VAR provides the best one-step-ahead point forecasts, but then the conventional VAR forecasts quite well at longer horizons. This is unsurprising given the results in the previous section. In particular, the impulse response functions in Figure 3 and Figure 4 suggested that the New Zealand real GDP response to uncertainty shocks is short-lived. The finding that the CSVM-VAR is superior only at a one-step-ahead horizon is therefore consistent with this result. Aside from these exceptions, the CSVM-VAR provides better point and density forecasts at all other horizons and strictly dominates the other models when forecasting inflation. Since each of these countries has an explicit inflation targeting mandate, the results are of practical significance to central bankers. In particular, by providing more accurate forecasts, accounting for uncertainty can aid policymakers in making better informed decisions.

Table 4: Forecasting results for Australia.

		RMSFE				MAE				ALPS				ACRPS			
Variable	Model	h=1	h=2	h=4	h=8	h=1	h=2	h=4	h=8	h=1	h=2	h=4	h=8	h=1	h=2	h=4	h=8
Real GDP	VAR	1.00	1.00	1.00	1.00	1.00	1.00	1.00	1.00	0.00	0.00	0.00	0.00	1.00	1.00	1.00	1.00
	CSV-VAR	0.97	0.95	0.96	0.99	0.95	0.92	0.94	0.98	0.06	0.10	0.13	0.11	0.96	0.93	0.93	0.95
	CSVM-VAR	0.97	0.93	0.95	0.99	0.96	0.90	0.93	0.98	0.11	0.15	0.16	0.16	0.97	0.93	0.94	0.95
Inflation	VAR	1.00	1.00	1.00	1.00	1.00	1.00	1.00	1.00	0.00	0.00	0.00	0.00	1.00	1.00	1.00	1.00
	CSV-VAR	0.99	0.97	0.97	0.97	0.96	0.96	0.96	0.97	0.01	0.01	0.00	0.00	0.97	0.96	0.97	0.98
	CSVM-VAR	0.97	0.95	0.95	0.98	0.94	0.93	0.90	0.95	0.12	0.14	0.13	0.16	0.97	0.96	0.96	0.96
Interest	VAR	1.00	1.00	1.00	1.00	1.00	1.00	1.00	1.00	0.00	0.00	0.00	0.00	1.00	1.00	1.00	1.00
	CSV-VAR	0.90	0.95	0.97	0.97	0.86	0.90	0.98	1.00	0.28	0.20	0.14	0.14	0.84	0.90	0.96	0.99
	CSVM-VAR	0.89	0.93	0.94	1.02	0.85	0.88	0.92	0.93	0.34	0.24	0.19	0.24	0.88	0.95	1.00	0.97

Table 5: Forecasting results for Canada.

		RMSFE				MAE				ALPS				ACRPS			
Variable	Model	h=1	h=2	h=4	h=8	h=1	h=2	h=4	h=8	h=1	h=2	h=4	h=8	h=1	h=2	h=4	h=8
Real GDP	VAR	1.00	1.00	1.00	1.00	1.00	1.00	1.00	1.00	0.00	0.00	0.00	0.00	1.00	1.00	1.00	1.00
	CSV-VAR	0.94	0.92	0.96	1.01	0.94	0.91	0.95	1.01	0.09	0.13	0.10	0.06	0.94	0.92	0.96	1.01
	CSVM-VAR	0.92	0.90	0.94	1.03	0.94	0.91	0.90	1.03	0.09	0.11	0.05	−0.01	0.95	0.93	0.99	1.09
Inflation	VAR	1.00	1.00	1.00	1.00	1.00	1.00	1.00	1.00	0.00	0.00	0.00	0.00	1.00	1.00	1.00	1.00
	CSV-VAR	0.96	0.92	0.96	0.91	0.95	0.91	0.95	0.91	0.07	0.11	0.05	0.10	0.96	0.92	0.96	0.89
	CSVM-VAR	0.90	0.87	0.94	0.95	0.88	0.86	0.89	0.91	0.12	0.14	0.00	0.03	0.92	0.89	0.96	0.96
Interest	VAR	1.00	1.00	1.00	1.00	1.00	1.00	1.00	1.00	0.00	0.00	0.00	0.00	1.00	1.00	1.00	1.00
	CSV-VAR	0.97	0.87	0.79	0.76	0.95	0.89	0.76	0.72	0.10	0.14	0.19	0.27	0.96	0.89	0.82	0.77
	CSVM-VAR	1.00	0.97	0.96	0.96	0.97	0.96	0.90	0.86	0.19	0.19	0.19	0.22	1.00	0.99	0.97	0.95

Table 6: Forecasting results for New Zealand.

		RMSFE				MAE				ALPS				ACRPS			
Variable	Model	h=1	h=2	h=4	h=8	h=1	h=2	h=4	h=8	h=1	h=2	h=4	h=8	h=1	h=2	h=4	h=8
Real GDP	VAR	1.00	1.00	1.00	1.00	1.00	1.00	1.00	1.00	0.00	0.00	0.00	0.00	1.00	1.00	1.00	1.00
	CSV-VAR	0.98	1.02	1.02	1.02	0.98	1.02	1.02	1.03	0.22	0.22	0.26	0.22	0.90	0.91	0.89	0.90
	CSVM-VAR	0.97	1.01	1.01	1.02	0.97	1.02	1.02	1.03	0.27	0.27	0.32	0.33	0.90	0.91	0.88	0.89
Inflation	VAR	1.00	1.00	1.00	1.00	1.00	1.00	1.00	1.00	0.00	0.00	0.00	0.00	1.00	1.00	1.00	1.00
	CSV-VAR	0.96	0.97	0.90	0.84	0.96	0.93	0.86	0.81	0.24	0.23	0.30	0.33	0.88	0.89	0.85	0.81
	CSVM-VAR	0.83	0.79	0.72	0.64	0.84	0.76	0.68	0.65	0.33	0.37	0.46	0.52	0.83	0.80	0.75	0.70
Interest	VAR	1.00	1.00	1.00	1.00	1.00	1.00	1.00	1.00	0.00	0.00	0.00	0.00	1.00	1.00	1.00	1.00
	CSV-VAR	0.91	0.92	0.90	0.87	0.92	0.94	0.94	0.92	0.25	0.20	0.18	0.19	0.87	0.89	0.89	0.88
	CSVM-VAR	0.89	0.89	0.82	0.76	0.96	0.96	0.91	0.82	0.27	0.23	0.25	0.30	0.90	0.92	0.87	0.80

5 Concluding Remarks and Future Research

Our objective in the paper was to estimate the effects of domestic and international sources of macroeconomic uncertainty in three commonly studied small open economies (SOEs): Australia, Canada and New Zealand. To this end, we proposed a common stochastic volatility in mean VAR (CSVM-VAR) model. To estimate the model we developed an efficient algorithm that built upon recent advances in band and sparse matrix algorithms. Our primary result was that both domestic and foreign sources of macroeconomic uncertainty shape the economic climate in each of the SOEs. In particular, international macroeconomic uncertainty spillovers were found to elicit a persistent negative effect on real GDP, while increasing both inflation and interest rates. Domestic uncertainty shocks were found to have a similar effect on inflation and interest rates, however the real GDP responses were idiosyncratic. In particular, the transmission of domestic uncertainty shocks in New Zealand was persistently positive while the Australian response is initially negative and becomes positive over time. This suggests that

these economies exhibit different transmission mechanisms compared to the US economy. More precisely, the New Zealand experience is suggestive of *growth options* or *Oi-Hartman-Abel* effects, while the Australian response is suggestive of a *precautionary savings* channel. This highlights a clear direction of future research: the investigation of such a channel within an estimated a small open economy DSGE model. Finally, in a forecasting exercise, the proposed model generally provided more accurate point and density forecasts compared to current benchmarks. Taken together, our results suggested that international uncertainty spillovers play a key role in shaping the macroeconomic environments in all SOEs and accounting for this uncertainty can aid policymakers in making better informed decisions.

A Appendix

A.1 Priors

In this Appendix we present the priors used in the empirical analysis in Section 3. To conduct the analysis, we set a Minnesota type prior for the VAR coefficients. In particular, the prior mean is set to a zero vector, $\boldsymbol{\beta}_0 = \mathbf{0}$, and the prior covariance matrix is diagonal with its corresponding elements set as follows:

$$\begin{aligned}
&\text{Var}(\mathbf{c}) = 10 \times \mathbf{I}_{2n}, \\
&\text{Var}(\mathbf{B}_l^{ij}) = \begin{cases} \frac{\lambda_1^2 \lambda_2}{l^{\lambda_3}} \frac{\sigma_i^2}{\sigma_j^2} & \text{for } l = 1, \ldots, p \text{ and } i \neq j, \\ \frac{\lambda_1^2}{l^{\lambda_3}} & \text{for } l = 1, \ldots, p \text{ and } i = j, \end{cases}
\end{aligned}$$

where $\mathbf{B}_l^{i,j}$ denotes the $(i,j)th$ element the matrix $\mathbf{B}_l$ and σ_r^2 is set equal to the variance the residual from AR(p) model for the variable r. The hyperparameters are set to be $\lambda_1 = 0.2$, $\lambda_2 = 0.5$, $\lambda_3 = 2$. We assume a relatively non-informative prior on the uncertainty impact matrix. To be specific, we set $\mathbf{a}_0 = \mathbf{0}$ and $\mathbf{V}_a = 5 \times \mathbf{I}_{2n}$. For the covariance matrix of the log volatilities, we set $\nu_h = 40$ and $\mathbf{S}_h = 0.1^2(\nu_h - n - 1) \times \mathbf{I}_n$. These values imply that the expected value of $\boldsymbol{\Sigma}_h$ is equal to $0.1^2 \times \mathbf{I}_n$. For the VAR coefficient matrix of the log-volatilities, we set $\boldsymbol{\phi}_0 = (0.9, 0, 0.9, 0)'$ and $\mathbf{V}_\phi = \mathbf{I}_2$. Lastly, for the variable-specific variance, we set $\eta_{i,L} = 10$, $\omega_{i,S} = 9$ for $i = 1, \ldots, n$, and $= \eta_{j,L} = 10$, $\omega_{i,L} = 9$ for $j = n+1, \ldots, 2n$. This implies that $\mathbb{E}(\sigma_{i,L}^2) = \mathbb{E}(\sigma_{j,S}^2) = 1$.

A.2 Gibbs Sampler

In this appendix we explain how to obtain draws from the conditional distributions in Steps 3-7 of the posterior simulator in Section 2.3. To this end, first note that equation (2)

can be written as

$$\mathbf{y}_t = \mathbf{X}_t\boldsymbol{\theta} + \boldsymbol{\epsilon}_t^y, \quad \boldsymbol{\epsilon}_t^y \sim \mathcal{N}(\mathbf{0}, \boldsymbol{\Sigma}_t) \tag{11}$$

where $\mathbf{X}_t = \left(\widetilde{\mathbf{X}}_t, \mathbf{W}_t, \mathbf{I}_{2n} \otimes (e^{h_t^L}, e^{h_t^S})\right)$ and $\boldsymbol{\theta} = (\boldsymbol{\beta}', \boldsymbol{\gamma}', \text{vec}(\mathbf{A}')')'$. Stacking the above equation over $t = 1, \ldots, T$, we get

$$\mathbf{y} = \mathbf{X}\boldsymbol{\theta} + \boldsymbol{\epsilon}^y, \quad \boldsymbol{\epsilon}^y \sim \mathcal{N}(\mathbf{0}, \boldsymbol{\Sigma}),$$

where $\mathbf{y} = (\mathbf{y}_1, \ldots, \mathbf{y}_T)'$, $\boldsymbol{\Sigma} = \mathbf{I}_{2n} \otimes \boldsymbol{\Sigma}_t$ and

$$\mathbf{X} = \begin{pmatrix} \mathbf{X}_1 \\ \vdots \\ \mathbf{X}_T \end{pmatrix}.$$

For Step 3 of the sampler, let $\mathbf{V}_{\boldsymbol{\theta}} = \text{diag}(\mathbf{V}_\beta, \mathbf{V}_\gamma, \mathbf{V}_a)$ and $\boldsymbol{\theta}_0 = (\boldsymbol{\beta}_0', \boldsymbol{\gamma}_0, \mathbf{a}_0')'$. Then, by standard results from linear regression, we have

$$\left(\boldsymbol{\beta}, \boldsymbol{\gamma}, \mathbf{A} | \mathbf{h}^L, \mathbf{h}^S, \boldsymbol{\Sigma}_L, \boldsymbol{\Sigma}_S, \mathbf{y}\right) \equiv \left(\boldsymbol{\theta} | \mathbf{h}^L, \mathbf{h}^S, \boldsymbol{\Sigma}_L, \boldsymbol{\Sigma}_S, \mathbf{y}\right) \sim \mathcal{N}\left(\widehat{\boldsymbol{\theta}}, \mathbf{D}_{\boldsymbol{\theta}}\right), \tag{12}$$

where $\mathbf{D}_{\boldsymbol{\theta}}^{-1} = \mathbf{X}'\boldsymbol{\Sigma}^{-1}\mathbf{X} + \mathbf{V}_{\boldsymbol{\theta}}^{-1}$ and $\widehat{\boldsymbol{\theta}} = \mathbf{D}_{\boldsymbol{\theta}}\left(\mathbf{X}'\boldsymbol{\Sigma}^{-1}\mathbf{y} + \mathbf{V}_{\boldsymbol{\theta}}^{-1}\boldsymbol{\theta}_0\right)$.

In Step 4, the full conditional distributions of the variance terms is standard. In particular, it follows that

$$\sigma_{i,L}^2 \sim \mathcal{IG}(\frac{T}{2} + \eta_{i,L}, \omega_{i,L} + \sum_{t=1}^{T} dy_{i,t}^2 e^{-h_t^L}), \quad i = 1, \ldots, n,$$
$$\sigma_{j,S}^2 \sim \mathcal{IG}(\frac{T}{2} + \eta_{j,S}, \omega_{j,S} + \sum_{t=1}^{T} dy_{j,t}^2 e^{-h_t^S}), \quad j = n+1, \ldots, 2n,$$

where $dy_{i,t}$ is the jth element of the vector $\mathbf{y}_t - \mathbf{X}_t\boldsymbol{\theta}$. Step 5 is essentially the same as

Step 4. Step 6 is also standard. In particular given the log volatilities, it follows that

$$(\boldsymbol{\Sigma}_h|\mathbf{h}^L,\mathbf{h}^S,\boldsymbol{\Phi}) \sim \mathcal{IW}(\widehat{\mathbf{S}}_h,\widehat{\nu}_h),$$

with $\widehat{\mathbf{S}}_h = \sum_{t=2}^{T}\mathbf{e}_t\mathbf{e}_t' + \mathbf{S}_h$ and $\widehat{\nu}_h = \nu_h + T - 1$, where

$$\mathbf{e}_t = \begin{pmatrix} h_t^L \\ h_t^S \end{pmatrix} - \boldsymbol{\Phi}\begin{pmatrix} h_{t-1}^L \\ h_{t-1}^S \end{pmatrix}.$$

For Step 7, we again apply standard linear regression results. In particular, we first note that the state equation can be expressed as

$$\mathbf{h}_t = \mathbf{X}_t^h\boldsymbol{\phi} + \boldsymbol{\epsilon}_t^h, \quad \boldsymbol{\epsilon}_t^h \sim \mathcal{N}(\mathbf{0},\boldsymbol{\Sigma}_h),$$

where $\mathbf{h}_t = (h_t^L, h_t^S)'$. Stacking all the state equations from $t = 2,\ldots,T$ that gives

$$\mathbf{h} = \mathbf{X}^h\boldsymbol{\phi} + \boldsymbol{\epsilon}^h, \quad \boldsymbol{\epsilon}^h \sim \mathcal{N}(\mathbf{0},\mathbf{I}_2\otimes\boldsymbol{\Sigma}_h).$$

Thus, the step 7 can be implemented as follows

$$(\boldsymbol{\Phi}|\mathbf{h}^L,\mathbf{h}^S,\boldsymbol{\Sigma}_h) \equiv (\boldsymbol{\phi}|\mathbf{h}^L,\mathbf{h}^S,\boldsymbol{\Sigma}_h) \sim \mathcal{N}(\widehat{\boldsymbol{\phi}},\mathbf{D}_\phi)1(\boldsymbol{\Phi}\in A),$$

where $\mathbf{D}_\phi^{-1} = \mathbf{X}^{h\prime}(\mathbf{I}_2\otimes\boldsymbol{\Sigma}_h)^{-1}\mathbf{X}^h + \mathbf{V}_\phi^{-1}$ and $\widehat{\boldsymbol{\phi}} = \mathbf{D}_\phi\left(\mathbf{X}^{h\prime}(\mathbf{I}_2\otimes\boldsymbol{\Sigma}_h)^{-1}\mathbf{h} + \mathbf{V}_\phi^{-1}\boldsymbol{\phi}_0\right)$. Since this full conditional distribution is not standard, we implement a Metropolis-Hasting step using $\mathbf{N}(\widehat{\phi},\mathbf{D}_\phi)$ as a proposal distribution.

References

K. A. Aastveit, H. C. Bjørnland, and L. A. Thorsrud. The world is not enough! Small open economies and regional dependence. *The Scandinavian Journal of Economics*, 118(1):168–195, 2016.

K. A. Aastveit, G. J. Natvik, and S. Sola. Economic uncertainty and the influence of monetary policy. *Journal of International Money and Finance*, 76:50–67, 2017.

A. B. Abel. Optimal investment under uncertainty. *The American Economic Review*, 73 (1):228–233, 1983.

C. Andrieu, A. Doucet, and R. Holenstein. Particle markov chain monte carlo methods. *Journal of the Royal Statistical Society: Series B*, 72(3):269–342, 2010.

S. R. Baker, N. Bloom, and S. J. Davis. Measuring economic policy uncertainty. *The Quarterly Journal of Economics*, 131(4):1593–1636, 2016.

R. Bansal and A. Yaron. Risks for the long run: A potential resolution of asset pricing puzzles. *The Journal of Finance*, 59(4):1481–1509, 2004.

S. Basu and B. Bundick. Uncertainty shocks in a model of effective demand. *Econometrica*, 85(3):937–958, 2017.

N. Bloom. The impact of uncertainty shocks. *Econometrica*, 77(3):623–685, 2009.

N. Bloom. Fluctuations in uncertainty. *Journal of Economic Perspectives*, 28(2):153–76, 2014.

N. Bloom, M. Floetotto, N. Jaimovich, I. Saporta-Eksten, and S. J. Terry. Really uncertain business cycles. *Econometrica*, 86(3):1031–1065, 2018.

B. Born and J. Pfeifer. Policy risk and the business cycle. *Journal of Monetary Economics*, 68:68–85, 2014.

G. Caggiano, E. Castelnuovo, and J. M. Figueres. Economic policy uncertainty spillovers in booms and busts. *Working Paper*, 2017.

F. Canova. The transmission of US shocks to Latin America. *Journal of Applied Econometrics*, 20(2):229–251, 2005.

F. Canova and M. Ciccarelli. ClubMed? Cyclical fluctuations in the Mediterranean basin. *Journal of International Economics*, 88(1):162–175, 2012.

F. Canova, M. Ciccarelli, and E. Ortega. Similarities and convergence in G-7 cycles. *Journal of Monetary Economics*, 54(3):850–878, 2007.

A. Carriero, T. E. Clark, and M. Marcellino. Common drifting volatility in large Bayesian VARs. *Journal of Business and Economic Statistics*, 34(3):375–390, 2016.

A. Carriero, T. E. Clark, and M. Marcellino. Measuring uncertainty and its impact on the economy. *Review of Economics and Statistics*, (Forthcoming), 2017.

A. Carriero, T. E. Clark, and M. Marcellino. Assessing international commonality in macroeconomic uncertainty and its effects. *Working Paper*, 2018.

J. C. Chan. The stochastic volatility in mean model with time-varying parameters: An application to inflation modeling. *Journal of Business and Economic Statistics*, 35(1): 17–28, 2017.

J. C. Chan and A. L. Grant. On the observed-data deviance information criterion for volatility modeling. *Journal of Financial Econometrics*, 14(4):772–802, 2016.

J. C. Chan and I. Jeliazkov. Efficient simulation and integrated likelihood estimation in state space models. *International Journal of Mathematical Modelling and Numerical Optimisation*, 1(1-2):101–120, 2009.

J. Cross, J. Chan, T. Kam, and A. Poon. Economic, Fiscal- or Monetary-policy Uncertainty Shocks: What Matters for a Small Open Economy? *Working Paper*, 2017.

R. Faccini, H. Mumtaz, and P. Surico. International fiscal spillovers. *Journal of International Economics*, 99:31–45, 2016.

J. Fernández-Villaverde, P. Guerrón-Quintana, K. Kuester, and J. Rubio-Ramírez. Fiscal volatility shocks and economic activity. *American Economic Review*, 105(11):3352–84, 2015.

J. Geweke and G. Amisano. Hierarchical Markov normal mixture models with applications to financial asset returns. *Journal of Applied Econometrics*, 26(1):1–29, 2011.

P. A. Guerron-Quintana. Common and idiosyncratic disturbances in developed small open economies. *Journal of International Economics*, 90(1):33–49, 2013.

R. Hartman. The effects of price and cost uncertainty on investment. *Journal of Economic Theory*, 5(2):258–266, 1972.

A. Ismailov and B. Rossi. Uncertainty and deviations from uncovered interest rate parity. *Journal of International Money and Finance*, 88:242–259, 2018.

E. Jacquier, N. G. Polson, and P. E. Rossi. Bayesian analysis of stochastic volatility models. *Journal of Business and Economic Statistics*, 20(1):69–87, 2002.

K. Jurado, S. C. Ludvigson, and S. Ng. Measuring uncertainty. *American Economic Review*, 105(3):1177–1216, 2015.

A. Justiniano and B. Preston. Can structural small open-economy models account for the influence of foreign disturbances? *Journal of International Economics*, 81(1):61–74, 2010.

S. Kim, N. Shephard, and S. Chib. Stochastic volatility: likelihood inference and comparison with ARCH models. *The Review of Economic Studies*, 65(3):361–393, 1998.

G. Koop, M. H. Pesaran, and S. M. Potter. Impulse response analysis in nonlinear multivariate models. *Journal of Econometrics*, 74(1):119–147, 1996.

S. J. Koopman and E. Hol Uspensky. The stochastic volatility in mean model: empirical evidence from international stock markets. *Journal of Applied Econometrics*, 17(6): 667–689, 2002.

R. E. Lucas. Econometric policy evaluation: A critique. In *Carnegie-Rochester Conference Series on Public Policy*, volume 1, pages 19–46. Elsevier, 1976.

W. J. McCausland. The HESSIAN method: Highly efficient simulation smoothing, in a nutshell. *Journal of Econometrics*, 168(2):189–206, 2012.

W. J. McCausland, S. Miller, and D. Pelletier. Simulation smoothing for state–space models: A computational efficiency analysis. *Computational Statistics and Data Analysis*, 55(1):199–212, 2011.

H. Mumtaz and K. Theodoridis. The international transmission of volatility shocks: An empirical analysis. *Journal of the European Economic Association*, 13(3):512–533, 2015.

H. Mumtaz and K. Theodoridis. The changing transmission of uncertainty shocks in the US. *Journal of Business and Economic Statistics*, pages 1–14, 2017a.

H. Mumtaz and K. Theodoridis. Common and country specific economic uncertainty. *Journal of International Economics*, 105:205–216, 2017b.

H. Mumtaz and F. Zanetti. The impact of the volatility of monetary policy shocks. *Journal of Money, Credit and Banking*, 45(4):535–558, 2013.

W. Y. Oi. The desirability of price instability under perfect competition. *Econometrica: Journal of the Econometric Society*, pages 58–64, 1961.

J. L. Paddock, D. R. Siegel, and J. L. Smith. Option valuation of claims on real assets: The case of offshore petroleum leases. *The Quarterly Journal of Economics*, 103(3): 479–508, 1988.

B. Rossi and T. Sekhposyan. Macroeconomic uncertainty indices based on nowcast and forecast error distributions. *American Economic Review*, 105(5):650–55, 2015.

H. Rue, S. Martino, and N. Chopin. Approximate Bayesian inference for latent Gaussian models by using integrated nested Laplace approximations. *Journal of the Royal Statistical Society: Series B*, 71(2):319–392, 2009.

S. Schmitt-Grohé. The international transmission of economic fluctuations:: Effects of US business cycles on the Canadian economy. *Journal of International Economics*, 44 (2):257–287, 1998.

N. Shephard and M. K. Pitt. Likelihood analysis of non-Gaussian measurement time series. *Biometrika*, 84(3):653–667, 1997.

C. A. Sims. Macroeconomics and reality. *Econometrica: Journal of the Econometric Society*, pages 1–48, 1980.

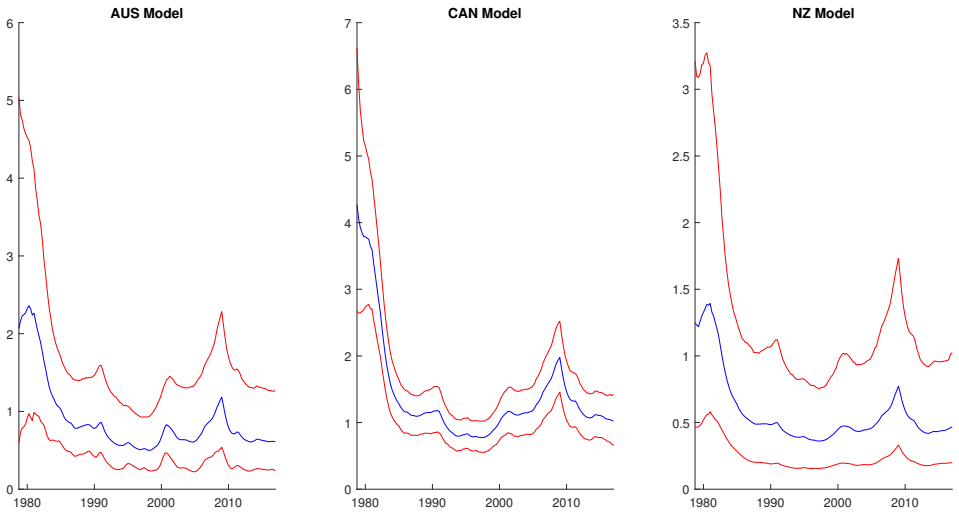

Figure 1: Uncertainty index for the US in each model: Australia (left), Canada (center) and New Zealand (right).

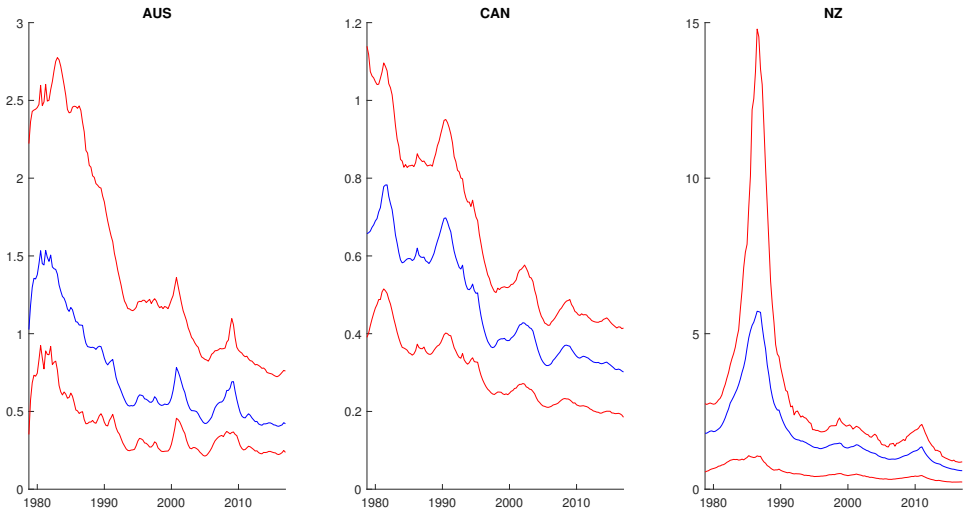

Figure 2: Uncertainty Index in small open economies: Australia (left), Canada (center) and New Zealand (right).

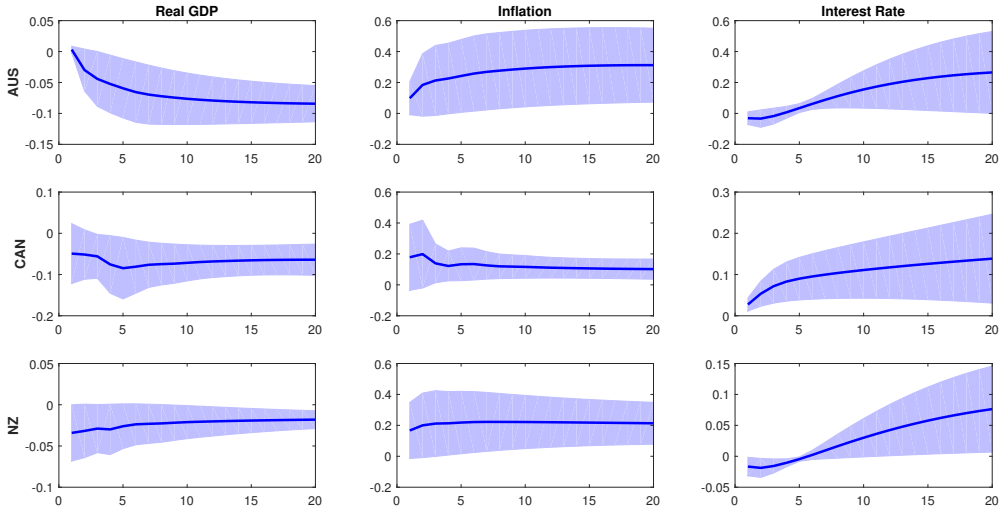

Figure 3: GIRF: 1 standard deviation uncertainty shock from the US: Australia (top row), Canada (center row) and New Zealand (bottom row).

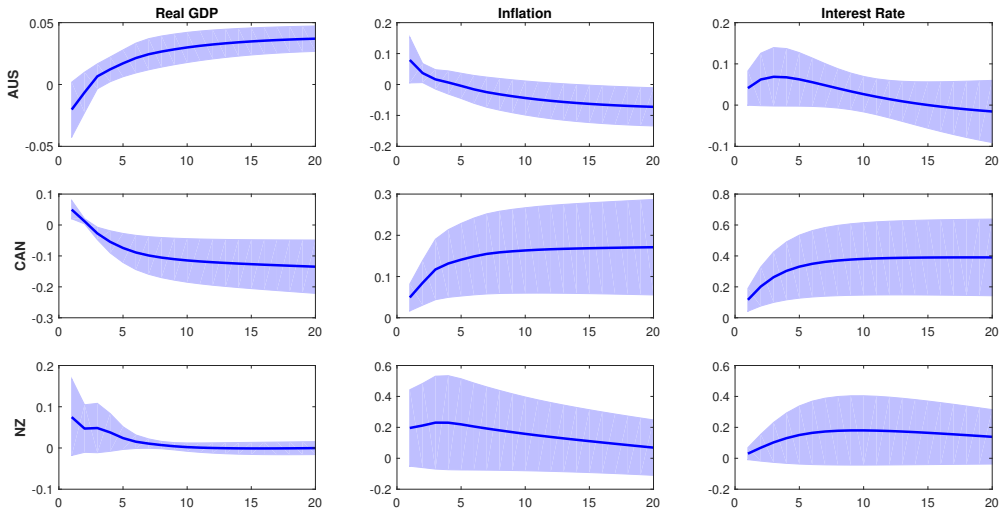

Figure 4: GIRF: 1 standard deviation domestic uncertainty shock from the SOE: Australia (top row), Canada (center row) and New Zealand (bottom row).

Centre for Applied Macroeconomics and Commodity Prices (CAMP)
will bring together economists working on applied macroeconomic issues, with special emphasis on petroleum economics.

BI Norwegian Business School
Centre for Applied Macroeconomics and Commodity Prices (CAMP)
N-0442 Oslo

http://www.bi.no/camp

CAMP Working Paper Series
ISSN: 1892-2198